TRANSFER OF THE MOMENTUM OF GAS IONS TO THE SURFACE OF A SOLID

V. A. Shuvalov

UDC 533.932-533.601.18

The thermal and force interaction between bodies and a flow of rarefied gas can be represented to a considerable extent by the momentum and energy exchange coefficients or by the equivalent accommodation coefficients. The accommodation coefficients are used when determining convective thermal fluxes and the aerodynamic characteristics of bodies under free molecular flow conditions, and are an important component of the theoretical relations irrespective of the model assumed for the interaction between the gas atoms and the surface of the solid.

The interaction between gas atoms with pure crystalline structures has been investigated very fully theoretically. There are a considerable number of publications devoted to numerical simulation of the collisions between atomic particles and the surface of a solid, and which contain approximate analytical solutions representing the mechanism of momentum and energy transfer between the atoms of gas and ideal crystal surfaces [1].

In practice, targets with an ideal single-crystal structure are encountered extremely rarely. In the majority of cases the bombarded targets have a polycrystalline structure, and the individual crystallites in these specimens are oriented at random. For a numerical investigation of the collisions between gas atoms with an atomically smooth polycrystalline surface it is necessary to average the interaction characteristics, which considerably complicates the problem [2]. There is insufficient information available on the theoretical and experimental values of the accommodation coefficients of gas molecules in the ~1-100 eV energy range, which is important from the aerodynamic point of view. It is therefore of considerable interest to investigate the interaction for different gas–surface systems in this particle-energy range.

In this paper we present the results of an experimental investigation of the effect of a number of factors representing the interaction between a gas and a surface on the value of the accommodation coefficients of the momentum of gas ions with an atomic mass from 4 to 131.

The momentum and energy fluxes transferred by the gas ions to an electrically conducting solid surface in a rarefied gas can be represented to a considerable extent by the accommodation coefficients of the energy α_i, the normal momentum σ_n, and the tangential momentum σ_t, and also by the work function $\varkappa$ of the surface material, and the secondary ion-electron emission coefficient γ_i.

In [3] relations were obtained from the energy-balance equation for points on the temperature characteristic $T_w = T_w(V)$ with equal temperatures for different potentials of a thermoanemometer probe, which establish a relationship between the parameters $\alpha_i, \varkappa, \gamma_i$. In [4] the effect of different factors on the energy transfer of gas ions to the surfaces of pure polycrystalline metals and technical alloys was investigated. To monitor the degree of purity of these surfaces the values of γ_i obtained from the data in [3] were used.

The force of a flow of rarefied plasma on a target depends very much on the potential of the solid surface. For positive target potentials with respect to the plasma potential ($V = \varphi_w - \varphi_0 > 0$) the force acting on the target due to the flow of low-density partially ionized gas is determined by the bombardment of the surface by electrons, and fast and slow neutrals, which occur due to recharging of the ions in the residual gas, metastable particles etc.

$$F_{V>0} = F_e + F_n + F_0 + F_m + \ldots = F_e(V) + \Delta F,$$

where F_e is the force due to electron bombardment, F_n is the contribution of fast neutrals, F_0 is the contribution of the residual gases, and F_m is the force due to metastables. For

Dnepropetrovsk. Translated from Zhurnal Prikladnoi Mekhaniki i Tekhnicheskoi Fiziki, No. 3, pp. 24-32, May-June, 1984. Original article submitted April 6, 1983.

0021-8944/84/2503-0351$08.50

negative potentials the target is subjected to a force due to bombardment of the surface by ions, neutrals, and metastables

$$F_{V<0} = F_i + F_n + F_0 + F_m + \ldots = F_i(V) + \Delta F,$$

where ΔF is independent of the target potential.

Taking into account the fact that the force due to bombardment of the surface by electrons is much less than the force due to ion bombardment [5],

$$\delta F = F_{V<0} - F_{V>0} = F_i - F_e \simeq F_i. \tag{1}$$

For an element of the surface or target in the form of a flat plate (a circular disk), the force due to the ionic component can be represented by the relations [6]

$$C_x\cos\theta + C_y\sin\theta = 2\cos\theta[p_1\sqrt{1+\eta^2} + (p_2 - 1)\sqrt{\cos^2\theta + \eta^2} + \cos\theta],$$
$$C_x\sin\theta - C_y\cos\theta = \sin 2\theta(\tau_1 + \tau_2\sqrt{\cos^2\theta + \eta^2/1 + \eta^2}).$$

On the other hand [1]

$$C_x\cos\theta + C_y\sin\theta = 2\cos\theta[(2 - \sigma_n)\cos\theta + \sigma_n\sqrt{\pi kT_w/4W_i}],$$
$$C_x\sin\theta - C_y\cos\theta = \sigma_t\sin 2\theta,$$

whence we obtain the following equations for the accommodation coefficients of the normal momentum σ_n and the tangential momentum σ_t:

$$\sigma_n = \frac{1 + [1 - e(F_x + F_y\,\mathrm{tg}\,\theta)\sqrt{2M_iW_i}I_i]/\sqrt{1+\eta^2/\cos^2\theta}}{1 - \sqrt{\pi kT_w(1+\eta^2)/4W_i(\cos^2\theta + \eta^2)}}, \tag{2}$$
$$\sigma_t = \frac{e(F_x - F_y\,\mathrm{ctg}\,\theta)}{\sqrt{2M_iW_iI_i}},$$

where F_x is the resistive force of the target, F_y is the lift in the ion flow, $\eta^2 = (e|V| + \chi)/W_i$; W_i is the energy transferred by the ions to the plasma-layer boundary surface, V is the potential difference through which the particles fall in the electrode layer, $I_i = I_{0i}\cos\theta$; I_{0i} is the ion saturation current to the probe when $\theta = 0$, $\chi = 3.6/d$ is the polarization energy, and d is the distance from the target surface at which neutralization of positive ions occurs. For the majority of surfaces and gas ions in the particle energy range considered $d \simeq 2\text{-}4\ \mathrm{mm}^{-7}$ [7]. With an error of not more than ~±10%, d can be obtained approximately as the half-sum of the diameter of a gas molecule, calculated from the viscosity, and the distance between the closest atoms of the target lattice [7].

Relations (1) and (2) enable one, using the current–voltage, temperature, and force characteristics of the target-probe, to determine the parameters of the force interaction between the ions of a flow of rarefied plasma and an electrically conducting surface. The resistance force F_x and the lift force of the target F_y in (2) are found from (1) for two points on the current–voltage characteristic of the plane probe: for a potential equal to the plasma potential, and for a target potential corresponding to the region of electron-current saturation. The position of these points corresponds to the two peaks on the electron branch of the current–voltage characteristic of a plane probe [8].

Experimental investigations to determine the interaction parameters of gas ions with the surfaces of electrically conducting materials were carried out on gas-dynamic plasma apparatus in a flow of partially ionized gas, generated by a gas-discharge accelerator in which the working material was ionized by electron collision. We used helium, neon, nitrogen, argon, krypton, and xenon of the highest purity as the working gases. The accelerated ion beam, having an intensity $j_\infty \simeq 10^{17}\ \mathrm{cm}^{-2}\cdot\mathrm{sec}^{-1}$, was admitted into the working chamber, in which the pressure of the residual gases was ~$(0.9\text{-}1.3) \times 10^{-4}$ Pa. Measurements were made at a pressure in the working chamber of ~$(1.16\text{-}2.1) \times 10^{-3}$ Pa. We used a target made in the form of a plane

thermoanemometer probe, a disk $\delta \approx 0.22$ mm with a diameter of the working surface of ~36 mm, to the rear side of which current leads and a miniature thermocouple were connected. The side and shadow surfaces of the disk and the thermocouple were coated with a heat-resistant dielectric (ceramic). Before carrying out the experiments the probe was first calibrated in a thermostat; the relationship $T_w = T_w(E)$ was determined, where E is the emf of the thermocouple.

The targets were made from pure polycrystalline metals with atomic mass from 27 to 207, and with a polished working surface (Al, Ti, Cu, Mo, Ta, W, and Pb), a chemically polished single-crystal disk of Si(III), and also from technical materials such as AMg6-BM and D16AT aluminum alloys (rolled), 12Kh18N10T and 2Kh13 stainless steels, steel 25, and an element from a solar-battery panel. Two probes were made from the solar-battery panel element (a plate with dimensions of 40 × 20 mm): a silicon element (a polished polycrystalline specimen of silicon with arsenic or phosphorous impurity), and a solder (lead–tin alloy; the shadow side of the panel). The surfaces of the targets made of technical materials corresponded to the working state of these materials [9].

The targets were set up on a compensation-type microbalance [10], based on a standard N359 dc milliammeter. We used the photodiode unit of an F359 dc amplifier operating with an N359 self-recording milliammeter as the tracking system. When using the microammeter of the magnetoelectric system the compensation current flowing through the frame of the instrument is directly proportional to the mechanical moment applied to it. A thin-walled aluminum tube 1.7 mm in diameter, the internal channel of which was used for the thermocouple elements, was employed as the holder-current-lead of the target. The external surface of the holder-current-lead was coated with a heat-resistant dielectric (enamel).

To increase the sensitivity of the microbalances, and to reduce the contribution of ΔF to the balance of the forces, the target holder was placed in a dielectric tube (glass) with an internal diameter of ~18 mm. In some cases, for the same purpose, the side and shadow sides of the target were screened from interaction with particles of the flow reaching the screen, which is at a potential equal to the target potential. The magnetoelectric system of the balances was screened from contact with the flow of rarefied plasma by a dielectric case. To eliminate any possible effect of vibrations, the balances were set up on a shock-resistant platform attached to a solid reference. When calibrating the microbalances we used the method described in [11]. The range of measured forces on the arm L ≈ 450 mm is $\sim 5 \times 10^{-3}$–250 dyn. The measurements were made automatically with synchronous recording of the current–voltage characteristic $I_\Sigma = I_\Sigma(V)$, the temperature characteristic $T_w = T_w(V)$, and the force characteristic $F_\Sigma = F_\Sigma(V)$.

The current–voltage characteristics were processed in the traditional way. The energy of the ions was determined using a multielectrode probe-analyzer. The plasma potential was found by the second-derivative method, and also from the electron part of the probe characteristic, drawn on a semilogarithmic scale. This determined the high accuracy of the measurements of the ion energy W_i, transferred by the particles to the plasma-layer boundary surface. The values of W_i, calculated assuming that the accelerating potential is equal to the difference between the potential of the source anode and the local plasma potential, agree satisfactorily with the data obtained using the multielectrode probe-analyzer. The spread in the values of W_i obtained does not exceed $\pm 4.5\%$. To monitor the local values of the flux parameters and the orientation of the target with respect to the flux velocity vector, we used a thin cylindrical probe made from molybdenum wire 0.04 mm in diameter and 2.3 mm long. The axis of the probe was parallel to the normal to the target surface. The peak of the ion current measured by this probe when rotated around the vertical or the horizontal axis corresponds to the orientation of the probe along the flow, and enables the degree to which the flow is nonisothermal to be estimated ($T_e/T_i \approx 7$–10 for $T_e \approx 4$ eV) [12].

The error in the angular orientation of the target in the flux did not exceed $\pm 20'$.

When making measurements, particular attention was given to the purity of the working surfaces of the targets. Before measurements were made the targets, at surface potentials $V \approx -250$ V, were subjected to preliminary bombardment by ions of the rarefied plasma for 10–15 min, after which for 15–20 min, as a result of electron bombardment, they were heated to temperatures at which no breakdown of the target material and thermocouple occurred. Then, the target was again subjected to a high negative potential $V \approx -250$ V, and for approximately 10 min immediately before measurements were made the working surfaces of the targets were aged

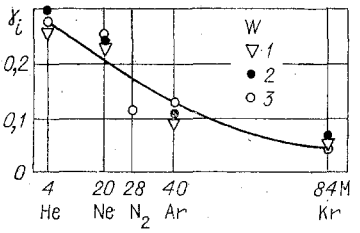

Fig. 1

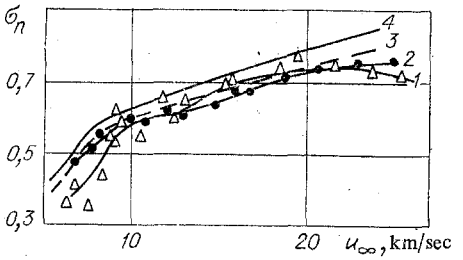

Fig. 2

by bombarding them with plasma. The current–voltage, temperature, and force characteristics were plotted beginning at V ≃ –250 V.

Information on the degree of purity of the surface investigated can be obtained from the results of measurements of the secondary-emission coefficient γ_i. The values of the work function obtained by bombarding the target with Xe^+ ions enabled us, using Eq. (4) from [3], to determine the secondary-emission coefficient γ_i of the ions of other gases. The values of the work function for pure-metal targets agree satisfactorily with the values of $\varkappa$ recommended in [13]. In addition to the data given in [3], we measured the work function of polycrystalline tungsten $\varkappa$ = 4.43 eV (Xe^+). The value of the work function of tungsten recommended in [13] is $\varkappa$ = 4.52 eV.

In Fig. 1 we show values of γ_i obtained when polycrystalline tungsten is bombarded with helium, neon, nitrogen, argon, and krypton ions with energies of ~100 eV. Points 1 correspond to the data in [14], points 2 correspond to the data in [15], and points 3 are the results of our measurements of γ_i. The values obtained hardly changed when the energy of the ions was varied in the range ~20–250 eV. This indicates the satisfactory state of the surface of the target investigated during the measurements.

Figure 2 illustrates the effect of the velocity of the particles bombarding the target on the value of the coefficient of normal momentum σ_n when θ = 0 (θ is the angle of attack of the target) for the N_2^+–Cu (μ = 0.441) system. Points 1 are the data from [16], curve 2 represents the results of our measurements, curve 3 shows the calculated values of σ_n on the surface of the solid, modeled by a linear harmonic oscillator, and curve 4 represents the results of a calculation of σ_n in which the collisions of the atoms of gas with a semiinfinite array of elastically bound atoms is numerically simulated using the data in [17] with μ = 0.5 and $\varepsilon_1 = E/\lambda\sigma^2 \simeq 0.001$. Here σ and E are the Lennard-Jones potential parameters, and λ is the elastic lattice constant of the target. When estimating the values of σ_n using the data given in [17], the characteristic temperature of Cu was taken to be $\Theta_{Cu} \simeq 32°K$ [18, 19]. The temperature of the target when measuring σ_n was $T_w \simeq 330$–$340°K$.

It should be noted that the results of the measurements of σ_n for the N_2^+–Cu system agree satisfactorily with the data obtained for σ_n for the Kr^+–W (μ = 0.457) and Kr^+–Ta (μ = 0.464) systems. In turn, the results of numerical estimates of σ_n for N_2^+–Cu (curves 3 and 4 in Fig. 2) agree satisfactorily with the calculated values of σ_n for Kr^+–W and Kr^+–Ta carried out taking into account the numerical data given in [17]. The results obtained confirm the preferential influence of the ratio of the atomic masses of the gas–metal system in this range of velocities.

The effect of μ (the mass ratio of the gas and target atoms) when the target is bombarded with atoms of mass from 27 to 207, and a single crystal of Si(III) is bombarded with Xe^+, Kr^+, Ar^+, N_2^+, Ne^+, and He^+ ions with $u_\infty \simeq 10$ km/sec and θ = 0 is illustrated more clearly in Fig. 3 (points 1–6 respectively). Points 7 represent the results of a calculation for the scattering of gas atoms by a plane square lattice [20], and points 8 represent the data

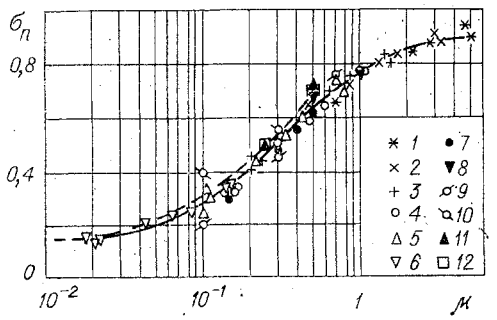

Fig. 3

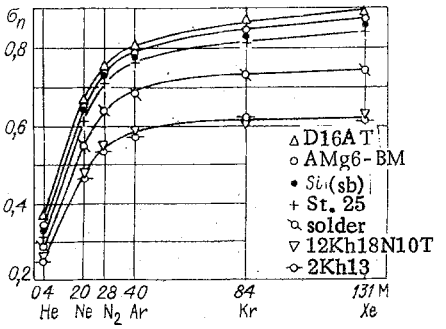

Fig. 4

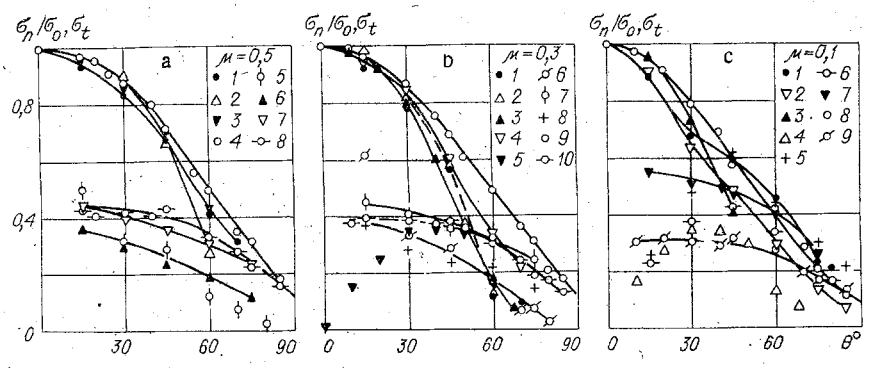

Fig. 5

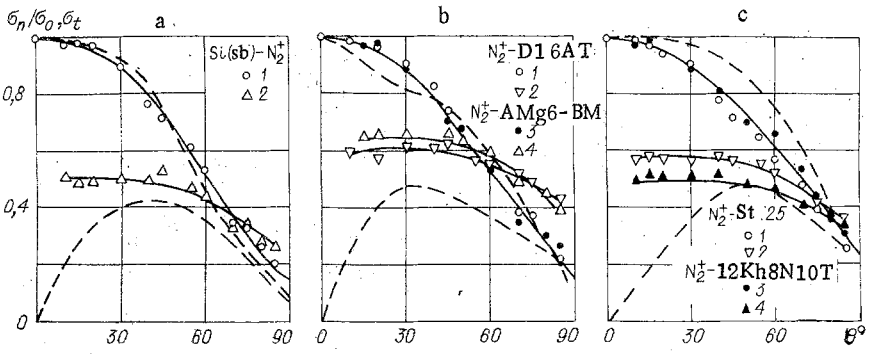

Fig. 6

obtained from calculations of the accommodation coefficients of the normal momentum when atomic particles interact with the surface of a solid modeled by a linear harmonic oscillator and a semiinfinite lattice of elastically bound atoms [17]. Points 9 and 10 represent the results of a numerical simulation of the interaction between the gas atoms and a three-dimensional crystal of interconnected atoms [21, 22]. Points 11 correspond to the calculated values of the accommodation coefficients of the normal momentum when gas atoms interact with the lattice of solid sphere [1] (taking into account the contribution of the first and second collisions), and points 12 represent the transfer of normal momentum of the gas atoms to an array of soft spheres [1].

The dashed lines represent the results of interpolation of the calculated values of σ_n for $\mu = 0$, 0.25, and 0.5, when atomic particles are scattered by a lattice of soft spheres [1].

The effect of the atomic mass of the gas ion bombarding the surface of targets of technical materials with $u_\infty \simeq 10$ km/sec and $\theta = 0$ on the value of σ_n is shown in Fig. 4.

Figure 5 illustrates the variation of σ_n/σ_0 and σ_t for inclined incidence of gas ions with a velocity $u_\infty \simeq$ km/sec with $\mu = 0.1$, 0.3, and 0.5 (σ_0 is the value of σ_n when $\theta = 0$). In Fig. 5a we show σ_n/σ_0 and σ_t as a function of the angle of attack on the target with $\mu \simeq 0.5$.

Curve 1 represents the results of a calculation of $\sigma_n(\theta)$ for scattering of gas atoms by a plane square lattice [20], curve 2 represents calculated values of σ_n when gas atoms are reflected from a lattice of solid spheres, taking into account the contribution of first and second collisions, points 3 represent the results of a calculation of the interaction between atomic particles with a lattice of soft spheres [1], and curve 4 shows the results of our measurements of $\sigma_n(\theta)/\sigma_0$ for the Kr^+—W system. The continuous curve, connecting points 4, illustrates the empirical relationship

$$\sigma_n/\sigma_0 \simeq \cos\theta + 0.333(1 + 1/\sigma_0)^{-1} \sin^2\theta |\sin^2\theta - \sqrt{\cos\theta}|. \quad (3)$$

Points 5 represent the results of a calculation of σ_t when gas atoms are reflected from a plane square lattice [20]. Curve 6 shows calculated values of the coefficient of tangential momentum when atomic particles interact with a lattice of soft spheres [1], and curve 7 represents calculated values of σ_t when gas atoms are reflected from a lattice of solid spheres [1]. The points on curve 8 represent the results of our measurements for the Kr^+—W system.

Figure 5b shows curves of $\sigma_n(\theta)/\sigma_0$ and $\sigma_t(\theta)$ for $\mu = 0.3$. Points 1 and 4 correspond to the results of a calculation for the scattering of atomic particles by a plane square lattice [20]. Curve 2 represents the calculated values of the coefficient of normal momentum when gas atoms interact with a lattice of soft spheres [1]. Curve 3 represents the results of a numerical simulation of the collisions of atomic particles with the surface of a solid taken from [22]. Points 5 show calculated values of the coefficient of tangential momentum [22]. Curve 6 illustrates the theoretical data in [20]. Points 7 represent the reflection of gas atoms from a lattice of solid spheres, and points 8 represent the reflection of gas atoms from a lattice of soft spheres [1]. Curves 9 and 10 represent our experimental data for (Ar^+—Mo). The continuous curve 9 represents the empirical relationship

$$\sigma_n/\sigma_0 \simeq \cos\theta + 0.333(1 + 1/\sigma_0)^{-1}\sin^2\theta(\sin^2\theta - \sqrt{\cos\theta}).$$

Figure 5c shows curves of $\sigma_n(\theta)/\sigma_0$ and $\sigma_t(\theta)$ for $\mu \simeq 0.1$. Curves 1 and 2 are the results of a calculation of σ_n when atomic particles interact with body-centered and face-centered lattices [23], and curve 3 represents the data given in [1, Fig. 17]. Points 4 are calculated values of σ_t from [22], and curves 5 and 6 are the results of a calculation of σ_t for body-centered and face-centered lattices of a three-dimensional crystal [23]. Curve 7 shows the data given in [1, Fig. 17], and curves 8 and 9 are the results of our measurements for Ne^+—W. The continuous curve for points 8 corresponds to the empirical approximation

$$\sigma_n/\sigma_0 \simeq \cos^{3/2}\theta + 0.333(1 + 1/\sigma_0)^{-1} \sin^2\theta \cos 2\theta.$$

In Fig. 6 we show the results of similar investigations carried out for N_2^+ ions on technical-alloy targets with $u_\infty \simeq 10$ km/sec. The dashed curves represent the results of calculations of $\sigma_n(\theta)/\sigma_0$ and $\sigma_t(\theta)$ of molecular nitrogen on a three-dimensional Si crystal, a crystal of Al and Cu alloy with a predominance of Al (with a composition close to D16AT), and on the surface of steel with different Cr and Ni contents (a composition close to 12Kh18N10T) with orbital velocities. The continuous curves for σ_n/σ_0 correspond to the empirical relationship (3).

A possible reason for the observed disagreement between the experimental and theoretical data for $\sigma_n(\theta)$ and $\sigma_t(\theta)$ for inclined incidence is the difference in the state of the surface of the atomically smooth ideal crystal targets, for which the numerical estimates were carried out, and the actual semicrystalline targets on which the experimental measurements were made. This is confirmed by the fact that for $\sigma_t(\theta)$ compared with $\sigma_n(\theta)$ the degree of observed disagreement increases, and the accommodation coefficient of the tangential momentum is more sensitive to the state of the bombarded surface.

TABLE 1

Gas	Xe^+	Kr^+	Ar^+	N_2^+	Ne^+	He^+
C_x^{Al} spheres	1,941	1,926	2,043	1,974	2,107	2,281

TABLE 2

Target material	Si(sb)	D16AT	AMg6-BM	Steel 25	12Kh18N10T
C_x spheres	1,882	1,981	2,019	1,962	2,042

It should be noted that the values of σ_n and σ_t measured for gas ions were compared with the results of calculations carried out for neutral particles. The problem of the extent to which the values of σ_n and σ_t measured for ions agree with the similar data for neutrals has been discussed in [7, 16]. The condition for such agreement in (2) is $\eta^2 \approx 0$. In the present paper, F_x and F_y were measured using (1) for target potentials equal to the plasma potential (V = 0). For such target potentials the difference in the interaction between the ion and neutral components with the surface of a solid is due to the effect of the electrical image force. For a rate of ion flow u_∞ = 10 km/sec for all the gas-surface systems considered, with the exception of the He^+—surface system, $\chi \ll W_i$. This is confirmed by the results of estimates carried out in [16] for $\sigma_n(N_2^+ - Cu)$. The results of measurements of C_x of an aluminum sphere 38 mm in diameter in a flow of rarefied He^+, Ne^+, N_2^+, Ar^+, Kr^+, and Xe^+ plasma with $u_\infty \approx 10$ km/sec (Table 1) confirms this estimate, as well as the results of calculations of C_x of a sphere made using the measured relationships $\sigma_n(\theta)$ and $\sigma_t(\theta)$ for aluminum alloys (Table 2). When calculating C_x of a sphere we took into account the change in the surface temperature of the targets investigated when measuring $\sigma_n(\theta)$ and $\sigma_t(\theta)$ from T_w =340°K (θ = 0) to T_w = 310°K ($\theta = \pi/2$). Calculations of C_x of a sphere agree satisfactorily with the results of similar calculations for different interaction schemes between atomic particles and a surface proposed in [24].

LITERATURE CITED

1. R. G. Barantsev, Interaction of Rarefied Gases with Surfaces [in Russian], Nauka, Moscow (1975).
2. Yu. A. Ryzhov and D. S. Strizhenov, "Interaction between the atoms of a gas and the surface of a solid," Zh. Prikl. Mekh. Tekh. Fiz., No. 4 (1967).
3. V. A. Shuvalov, N. P. Reznichenko, and A. V. Gavrilov, "Investigation of the parameters of the interaction between a flow of rarefied plasma with electrically conducting surfaces using thermoanemometer probes," Teplofiz. Vyssh. Temp. 19, No. 3 (1981).
4. V. A. Shuvalov, "Accommodation of gas-ion energy on the surface of polycrystalline materials," Zh. Prikl. Mekh. Tekh. Fiz., No. 6 (1983).
5. A. V. Gurevich and A. M. Moskalenko, "The slowing down of solids moving in a rarefied plasma," in: Investigation of Cosmic Space [in Russian], Nauka, Moscow (1965).
6. A. P. Kuryshev and B. V. Filippov, "Aerodynamic coefficients of solids of rotation in an extremely rarefied plasma," in: Aerodynamics of Rarefied Gases, No. 4 [in Russian], Izd. Leningr. Univ., Leningrad (1969).
7. B. V. Filippov, "Interaction of gas ions with the surface of a metal," in: Aerodynamics of Rarefied Gases, No. 3, Izd. Leningr. Univ., Leningrad (1967).
8. S. J. Weber, R. J. Armstrong, and J. Trulsen, "Ion-beam diagnostics by means of an electron-saturated plane Langmuir probe," J. Appl. Phys., 50, No. 7 (1979).
9. V. M. Kovtunenko, V. F. Kameko, and É. P. Yaskevich, Aerodynamics of Orbital Cosmic Apparatus [in Russian], Naukova Dumka, Kiev (1977).

10. D. G. Marsden, "Average-sensitivity microbalances for measuring the pressure forces of molecular beams," Prib. Nauch. Issled., 39, No. 1 (1968).
11. A. P. Gritsenko and I. N. Magda, "Microbalances with a capacitor probe with bent plates," Prib. Tekh. Eksp. No. 5 (1966).
12. V. A. Shuvalov and V. V. Gubin, "Determination of the degree of departure from isothermal conditions in a flow of rarefied plasma by probe methods," Teplofiz. Vys. Temp., 16, No. 4 (1978).
13. V. S. Fomenko and I. A. Podchernyaeva, Emission and Adsorption Properties of Materials [in Russian], Atomizdat, Moscow (1975).
14. M. Kaminskii, Atomic and Ionic Collisions on Metal Surfaces [in Russian], Mir, Moscow (1967).
15. U. A. Arifov, Interaction between Atomic Particles and Solid Surfaces [in Russian], Nauka, Moscow (1968).
16. W. N. Mair, B. W. Viney, and J. S. Colligon, "Experiments on the accommodation of normal momentum," in: Rarefied Gas Dynamics, Vol. 1, Academic Press, New York (1967).
17. A. I. Erofeev and A. V. Zhbakova, "Calculation of the collisions between the atoms of a gas and a surface for different models of a solid," Uchen. Zap. TsAGI, 3, No. 5 (1972).
18. C. Kittel, Introduction to Solid-State Physics, 4th edn., Wiley (1971).
19. L. Zhirifal'ko, Statistical Solid-State Physics [Russian translation], Mir, Moscow (1975).
20. A. I. Erofeev, "Energy and momentum exchange between atoms and molecules of a gas and a solid surface," Zh. Prikl. Mekh. Tekh. Fiz., No. 2 (1967).
21. A. A. Pyarnpuu, "Calculation of the interaction between a single-energy beam of gas atoms and a three-dimensional crystal," Zh. Prikl. Mekh. Tekh. Fiz., No. 2 (1970).
22. A. A. Pyarnpuu, "Models of the interaction between a rarefied gas and a surface," in: Numerical Methods in the Theory of Rarefied Gases [in Russian], VTs Akad. Nauk SSSR, Moscow (1969).
23. A. A. Pyarnpuu, "Computer study of gas atoms scattering from a solid surface with application to calculation of satellite drag coefficient," Entropic, No. 42 (1971).
24. V. P. Bass, "Calculation of the flow of an extremely rarefied gas around a solid taking interaction with the surface into account," Izv. Akad. Nauk SSSR, Mekh. Zhidk. Gaza, No. 5 (1978).

PULSED PERIODIC GAS DISCHARGE IN A CHAMBER WITH A HELMHOLTZ RESONATOR

A. V. Gubarev, A. A. Nekrasov,
and N. K. Novikova

UDC 533.534-13

It was pointed out in [1, 2] that thermal energy released in a gas discharge chamber of a pulsed periodic CO_2 laser with a Helmholtz resonator might be used to excite nonlinear oscillations in the resonator, and consequently to realize wave self-pumping of a gas mixture. This suggestion was based on practical realizations of pulsed air-breathing jet engines and a pulsating combustion chamber with a Helmholtz resonator [3, 4], and also on theoretical estimates and direct numerical experiment [1, 2]. Since the flow discharge of a pulsed periodic CO_2 laser requires rather uniform parameters of the gas in the discharge chamber, relatively low specific energy inputs etc., the conclusions in [1, 2] require direct experimental verification. In the present article we report preliminary results of such an experiment.

The experiments on wave pumping of a gas mixture by exciting nonlinear oscillations in a Helmholtz resonator were performed on the arrangement shown schematically in Fig. 1. The 0.5 × 0.3 × 0.3 m sealed chamber 1 contained a Helmholtz resonator with a rectangular neck 7, 0.035 × 0.07 m in cross section and 0.3 m long, and the 1000-cm^3 vessel 9. The discharge chamber 14 with electrodes 5 and 15 was located in the neck of the resonator in the immediate

Moscow. Translated from Zhurnal Prikladnoi Mekhaniki i Tekhnicheskoi Fiziki, No. 3, pp. 32-34, May-June, 1984. Original article submitted March 24, 1983.

0021-8944/84/2503-0358$08.50